Available online at www.sciencedirect.com

SciVerse ScienceDirect

www.elsevier.com/locate/brainres

BRAIN RESEARCH

Research Report

Projections from the anteroventral part of the medial amygdaloid nucleus in the rat

*Leonardo S. Novaes, Sara J. Shammah-Lagnado**

Department of Physiology and Biophysics, Institute of Biomedical Sciences, University of São Paulo, São Paulo, SP 05508-900, Brazil

ARTICLE INFO

Article history:
Accepted 10 September 2011
Available online 17 September 2011

Keywords:
Accessory olfactory bulb
Amygdala
Amygdalostriatal transition area
Ventromedial hypothalamic nucleus
Defensive behavior

ABSTRACT

The medial amygdaloid nucleus (Me) integrates pheromonal and olfactory information with gonadal hormone cues, being implicated in social behaviors. It is divided cytoarchitectonically in an anterodorsal, anteroventral (MeAV), posterodorsal and posteroventral part, whose projections are well characterized, except for those of the tiny MeAV. Here, MeAV efferents were examined in the rat with the anterograde *Phaseolus vulgaris* leucoagglutinin (PHA-L) and retrograde Fluoro-Gold (FG) tracers and compared with those of other Me parts. The present PHA-L observations show that the MeAV projects profusely to itself, but its projections to other Me parts are modest. In conjunction with FG experiments, they suggest that the MeAV innervates robustly a restricted set of structures it shares with the anterodorsal and/or posteroventral Me. Its major targets are the core of the ventromedial hypothalamic nucleus (especially the dorsomedial and central parts), reached mainly via the stria terminalis, and the amygdalostriatal transition area. In addition, the MeAV innervates substantially the lateral and posterior basomedial amygdaloid nuclei and the intraamygdaloid bed nucleus of the stria terminalis. In contrast to other Me parts, it provides only modest inputs to the main and accessory olfactory systems, medial bed nucleus of the stria terminalis and reproductive hypothalamic nuclei. This anatomical framework suggests that the MeAV may play a role in orienting responses to chemosensory cues and defensive behaviors elicited by the odor of predators.

1. Introduction

The medial amygdaloid nucleus (Me) integrates chemosensory signals from the vomeronasal and main olfactory systems with gonadal steroid hormone cues (Canteras et al., 1995; Gomez and Newman, 1992; McDonald, 1998; Pro-Sistiaga et al., 2007; Swanson and Petrovich, 1998) and is thought to play a key role in social behaviors (Choi et al., 2005; Kollack-Walker and Newman, 1995; Newman, 1999), including social learning and memory (Luiten et al., 1985), as well as in innate anti-predatory defensive responses (Canteras et al., 2001; Dielenberg et al., 2001; Martinez et al., 2011).

The Me is divided cytoarchitectonically in an anterodorsal (MeAD), anteroventral (MeAV), posterodorsal (MePD) and posteroventral part (MePV) (Paxinos and Watson, 2007). This parceling is also supported by the selective expression of members of the conserved family of LIM homeodomain genes (Choi et al., 2005). In particular, the Lhx5 gene occupies a well-demarcated region, which corresponds roughly to the MeAV. Other neurochemical attributes further differentiate the MeAV from the rest of Me, such as a high density of glutamatergic (Poulin et al., 2008) and nitric oxide producing neurons (McDonald et al., 1993) allied to a virtual absence of gamma amino butyric acid (GABA)ergic neurons (Poulin et al., 2008).

* *Corresponding author*. Fax: +55 11 3091 7285.
E-mail address: sara@icb.usp.br (S.J. Shammah-Lagnado).

0006-8993
doi:10.1016/j.brainres.2011.09.021

The major features of Me connectivity have long been established and differences between the anterior Me, primarily dependent on chemosensory inputs, and the MePD, heavily interconnected with gonadal steroid-responsive brain regions, are widely acknowledged (Canteras et al., 1995; Coolen and Wood, 1998; Gomez and Newman, 1992). Canteras et al. (1995), in a comprehensive study in the rat using the sensitive *Phaseolus vulgaris* leucoagglutinin (PHA-L) anterograde tracer, described in detail the projections arising from the MeAD, MePV and MePD, but the projections of the MeAV, due to the small size of this division, were not thoroughly examined. They noted however, that injections encompassing the MeAV and MeAD produced a dense terminal field in the core region of the ventromedial hypothalamic nucleus (dorsomedial and central divisions), whereas injections restricted to the MeAD labeled primarily the shell region. In consonance with Canteras et al. (1995), Choi et al. (2005) reported in mice that MeAV neurons are retrogradely labeled after injections into hypothalamic nuclei (the anterior nucleus and dorsomedial part of the ventromedial nucleus) associated with defensive behavior (Canteras et al., 2001; Swanson, 2000).

In the present study, MeAV projections will be documented based on the analysis of a case with an injection of PHA-L virtually confined to the MeAV and control cases in which injections of the retrograde tracer Fluro-Gold (FG) were placed in major terminal fields of the Me.

2. Results

2.1. *Anterograde tracing experiments*

2.1.1. *Injection sites*

A total of 14 cases with PHA-L injections in the Me were examined, 4 of them (516, 517, 564 and 565) extracted from a library of cases. One injection (case 565; Figs. 1 and 2) is almost confined to the tiny MeAV, two were located in the MeAD (cases 516 and 517; Fig. 2), one (case 564) involved both the MeAD and MeAV, and six (cases 758, 765, 788, 790, 791 and 798; Fig. 2) were primarily in the MePV. The remaining injections encompassed to a variable extent the MeAD, MePV and/or MePD.

2.1.2. *Case 565*

This case had an injection in the MeAV with only a few PHA-L labeled neurons in the MeAD (Figs. 1 and 2A). Efferents issued from the MeAV are almost exclusively ipsilateral and innervate substantially a restricted set of structures, their main target being the core region of the ventromedial hypothalamic nucleus (Fig. 3).

Many labeled fibers with closely spaced varicosities were seen in the MeAV (Fig. 4A) and a light to moderately dense terminal labeling was observed in the other divisions of the Me, being more pronounced in the MePV (Figs. 3E–H, 4B). A group of fibers extending caudally from the injection site innervates very substantially the amygdalostriatal transition area (Figs. 3F–H, 5A) and moderately, the lateral amygdaloid nucleus (mainly the ventrolateral division, but also the ventromedial division), posterior basomedial amygdaloid nucleus and intraamygdaloid part of the bed nucleus of the stria terminalis (BST; Figs. 3G–J, 5). Varicose fibers could also be traced into the posterior part of the capsular division of the central nucleus, which otherwise is sparingly labeled (Figs. 3E–G). A modest terminal labeling was noted in the posterolateral and posteromedial cortical nuclei, becoming more expressive caudally (Figs. 3G–K). The basolateral nucleus is free of labeling, except for some varicose axons in the lateral part of the posterior division (Fig. 3G). The anterior amygdaloid area and anterior basomedial amygdaloid nucleus are traversed by unbranched fibers with occasional bouton-like swellings, interpreted as fibers-of-passage (Figs. 3E and F).

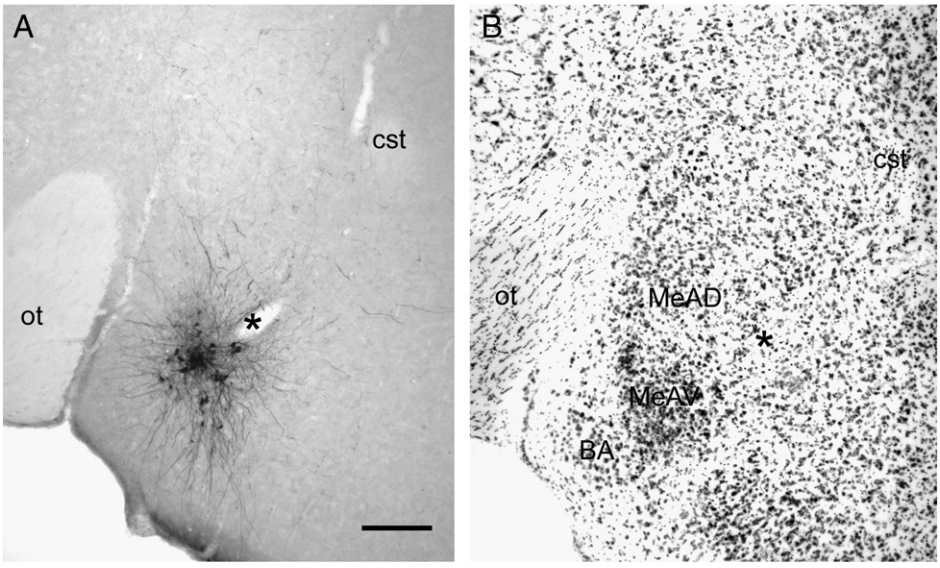

Fig. 1 – Brightfield photomicrographs showing a PHA-L injection site in the anteroventral part of the medial amygdaloid nucleus (MeAV; case 565) and the adjacent Nissl-stained section. *Indicates the same blood vessel. BA, bed nucleus of the accessory olfactory tract; cst, stria terminalis, commissural component; MeAD, medial amygdaloid nucleus, anterodorsal part; ot, optic tract. Scale bar = 200 μm.

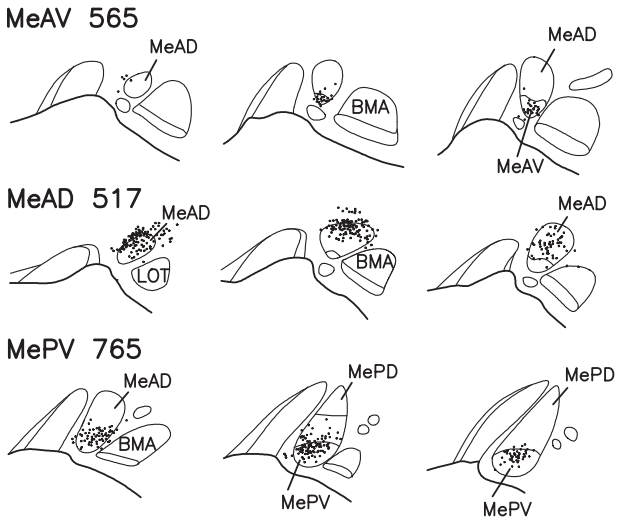

Fig. 2 – Camera lucida plots of PHA-L injection sites in different parts of the medial amygdaloid nucleus. Sections are arranged from rostral (left) to caudal (right). Dots indicate PHA-L-immunoreactive cell bodies. BMA, anterior basomedial amygdaloid nucleus; LOT, nucleus of the lateral olfactory tract; MeAD, medial amygdaloid nucleus, anterodorsal part; MeAV, medial amygdaloid nucleus, anteroventral part; MePD, medial amygdaloid nucleus, posterodorsal part; MePV, medial amygdaloid nucleus, posteroventral part.

Labeled fibers coursing through the amygdala reach the piriform cortex, amygdalopiriform transition area and lateral entorhinal cortex, all of them sparsely labeled (Figs. 3E–L). Rostrally, the agranular insular cortex displays a modest terminal field in the posterior part (Fig. 3B).

The major contingent of labeled fibers issued from the injection site travels in the medial part of the stria terminalis (Fig. 3D) and a more modest stream incorporates to the ansa peduncularis, generating along its course a light terminal field in the medial sublenticular extended amygdala (Fig. 3D). These two fiber paths merge in the posterior part of the BST. They originate light to moderately dense projections to the anterior, ventral and posterolateral parts of the medial BST and almost completely avoid the posteromedial part (Figs. 3B, C, 6A, C). Remarkably, tiny highly varicose terminal fields apposed to the wall of the lateral ventricle were observed in the rostrodorsal extent of the BST (Fig. 3A) and in a cell-poor district, located lateral to the small densely-packed dorsal nucleus of Ju and Swanson (1989)—also designated subventricular nucleus (Moga et al., 1989)—and seemingly pertaining to the strial extension of the BST (Ju and Swanson, 1989) (Figs. 3B and 6A). Rostral to the BST, the anterograde labeling becomes very sparse. Few labeled fibers were seen in the olfactory tubercle, ventral border of the nucleus of the horizontal limb of the diagonal band, fundus striati, caudal accumbens, lateral septal nucleus (Figs. 3A and B), infralimbic cortex and anterior olfactory nucleus. The accessory olfactory bulb is devoid of labeling.

Fibers from the posterior BST proceed ventrocaudally in the direction to the hypothalamus to innervate very lightly, at the preoptic anterior hypothalamic level, the rostral part of the medial preoptic nucleus and medial preoptic area (Figs. 3B and C) and, more substantially, the retrochiasmatic area (Fig. 3D). Labeled fibers in the anterior hypothalamic nucleus have largely spaced varicosities and seemingly provide only a sparse input to this nucleus (Figs. 3C–E). A few fibers were found in the periventricular zone including the paraventricular nucleus, which shows a modest number of terminals in the anterior parvo- and magnocellular parts (Figs. 3C and D).

At the tuberal level, the MeAV provides a particularly dense input to the dorsomedial and central parts of the ventromedial nucleus, but the anterior and ventrolateral parts are also labeled (Figs. 3E–G, 7A). Curiously, the caudal extent of the ventrolateral part, which in Nissl-stained sections shows more densely-packed and darkly-stained neurons than the rest of the ventrolateral part (Coolen et al., 1996), is almost completely avoided. Terminal labeling was also observed in the subfornical region of the lateral hypothalamus, but ventral to it, the tuberal nucleus is sparsely labeled (Figs. 3F,G, 7A). In addition, a few varicose axons were found in the dorsomedial hypothalamic nucleus and intermediate periventricular nucleus (Figs. 3F–H).

At the mammillary level, a rather modest terminal field was observed in the ventral premammillary nucleus and a lighter one in the ventrolateral part of the dorsal premammillary nucleus (Figs. 3I, J, 7C). Some varicose fibers were also noted in the posterior periventricular nucleus, lateral hypothalamic area (Fig. 3I) and, still fewer, in the posterior hypothalamic nucleus and supramammillary region (Figs. 3I–K, 7C). Some labeled fibers enter the periventricular gray to innervate very lightly the dorsolateral periaqueductal gray (Fig. 3L) and dorsal raphe nucleus. Only occasional fibers were found in the nucleus reuniens, paraventricular nucleus and mediodorsal nucleus of the thalamus.

A few labeled fibers cross the midline in the anterior, supraoptic and posterior commissures and in the supramammillary region. The ventromedial hypothalamic nucleus is the sole structure on the contralateral side of the brain which shows an appreciable number of terminals (Figs. 3F–G).

2.1.3. *Other cases*

The pattern of anterograde labeling observed after injections in the MeAD and MePV is similar to that described in male rats by Canteras et al. (1995). We will pinpoint only specific aspects that are relevant for a comparison with the MeAV case 565. 1) The minor spread of the injection into the MeAD does not seem to have affected significantly the distribution of anterograde labeling in case 565, as inferred by the virtual absence of labeling in major MeAD projection fields, such as the accessory olfactory bulb, nucleus of the horizontal limb of the diagonal band, olfactory tubercle and nucleus reuniens (Canteras et al., 1995; de Olmos et al., 1978; present observations). 2) MeAV projections to other Me parts, medial sublenticular extended amygdala and medial BST, continuum referred to as the medial extended amygdala (Alheid and Heimer, 1988; de Olmos and Heimer, 1999), are much less dense than those from the MeAD or MePV (Figs. 4 and 6). Varicose foci in BST subventricular districts (Figs. 3A, B, 6A, B) were observed only after injections involving the MeAV (cases 564 and 565 and case 6 from Dr. Newton S. Canteras collection). 3) The

MeAV, MeAD and MePV have similar projections to the ventral part of the lateral amygdaloid nucleus and posterior basomedial amygdaloid nucleus, but only the MeAV and MeAD target the amygdalostriatal transition area. On the other hand, MeAV projections to the main olfactory system are less dense and widespread than those from the MeAD or MePV. 4) Projections from the MeAV and MePV to the core region of the ventromedial hypothalamic nucleus have a similar distribution and density (Fig. 7). However, in contrast to the MeAV, the MePV innervates very robustly the shell of the ventromedial hypothalamic nucleus, the intermediate periventricular nucleus and the tuberal nucleus (Fig. 7B). 5) The MeAD and MePV provide considerably denser inputs to the medial preoptic and ventral premammillary nuclei, key components of the reproductive hypothalamic network (Simerly, 2002; Swanson, 2000) than does the MeAV (Figs. 3B, C, 7C, D).

2.2. *Retrograde tracing experiments*

2.2.1. *Injection sites*

To confirm the present anterograde tracing observations, injections of FG were placed in regions which were found to be substantially labeled in MeAV case 565 or in regions which, albeit sparingly labeled in MeAV case 565, are known to receive major inputs from other Me parts. The injection sites of representative cases of the different prosencephalic regions that were explored in the present work are illustrated in Fig. 8. One injection (case 181) was located in the caudal half of the lateral amygdaloid nucleus and did not spread over the amygdalostriatal transition area. Two injections (cases 737 and 738) were restricted to the posterior basomedial amygdaloid nucleus. One injection (case 740) encompassed the amygdalostriatal transition area and the lateral part of the central amygdaloid nucleus,

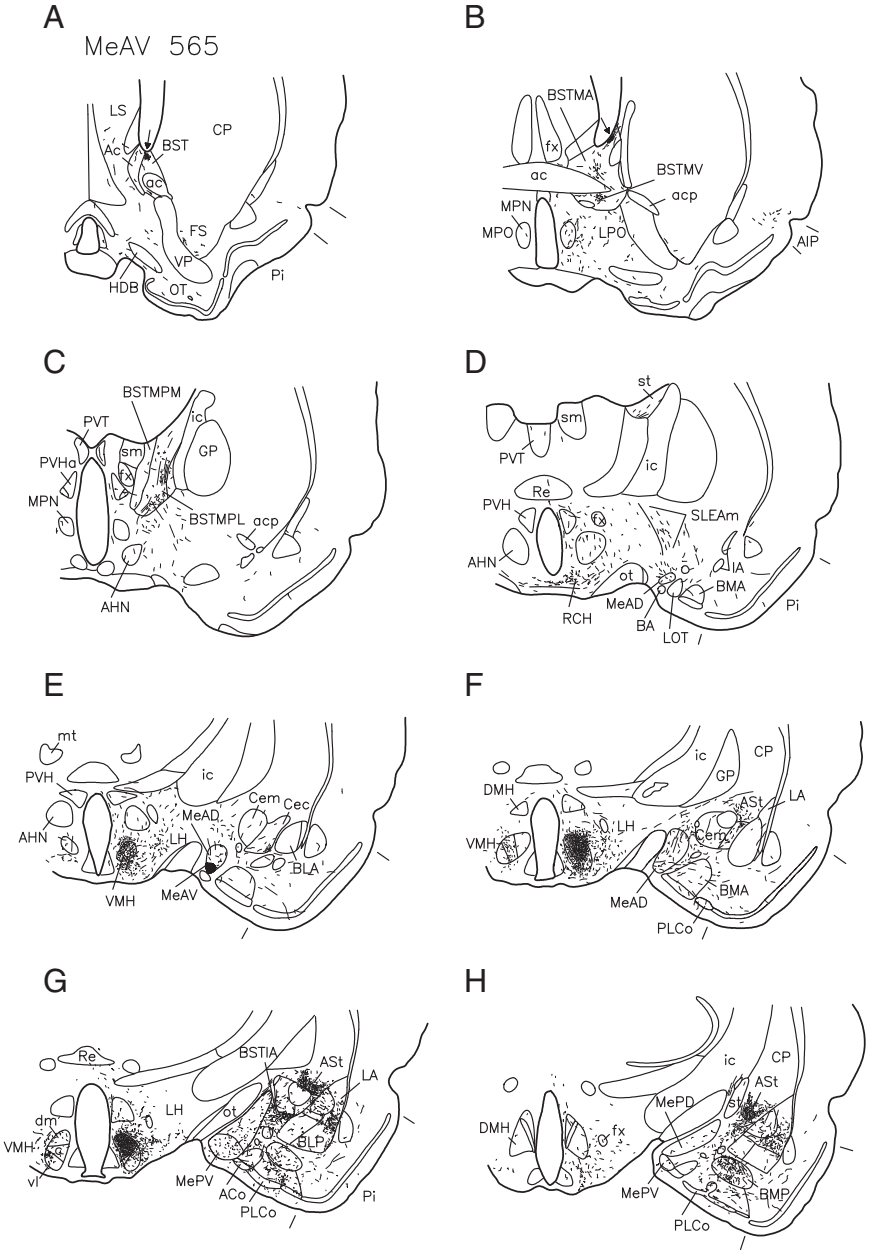

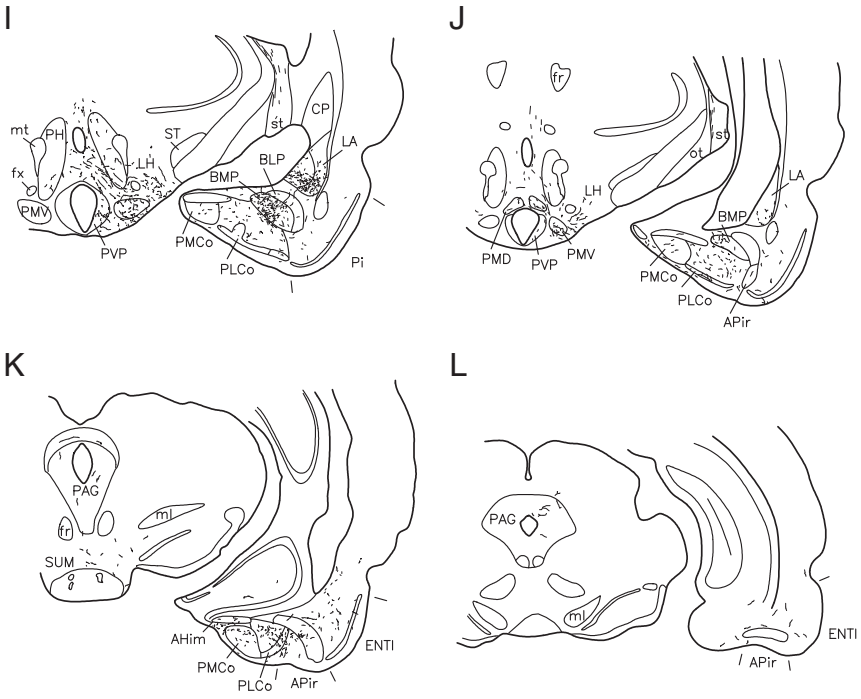

Fig. 3 – Distribution of PHA-L-labeled fibers after an injection in the MeAV (case 565). The black area in E indicates the injection site. Arrows in A and B point to small varicose foci in the BST apposed to the lateral ventricle. Ac, accumbens; ac, anterior commissure; ACo, anterior cortical amygdaloid nucleus; acp, anterior commissure, posterior limb; AHim, amygdalohippocampal area, medial part; AHN, anterior hypothalamic nucleus; AIP, agranular insular cortex, posterior part; APir, amygdalopiriform transition area; ASt, amygdalostriatal transition area; BA, bed nucleus of the accessory olfactory tract; BLA, anterior basolateral amygdaloid nucleus; BLP, posterior basolateral amygdaloid nucleus; BMA, anterior basomedial amygdaloid nucleus; BMP, posterior basomedial amygdaloid nucleus; BST, bed nucleus of the stria terminalis; BSTIA, bed nucleus of the stria terminalis, intraamygdaloid part; BSTMA, medial bed nucleus of the stria terminalis, anterior part; BSTMV, medial bed nucleus of the stria terminalis, ventral part; BSTMPL, medial bed nucleus of the stria terminalis, posterolateral part; BSTMPM, medial bed nucleus of the stria terminalis, posteromedial part; Cec, central amygdaloid nucleus, capsular part; Cem, central amygdaloid nucleus, medial part; CP, caudate-putamen; DMH, dorsomedial hypothalamic nucleus; ENTl, lateral entorhinal cortex; fr, fasciculus retroflexus; FS, fundus striati; fx, fornix; GP, globus pallidus; HDB, nucleus of the horizontal limb of the diagonal band; IA, intercalated amygdaloid nuclei; ic, internal capsule; LA, lateral amygdaloid nucleus; LH, lateral hypothalamic area; LOT, nucleus of the lateral olfactory tract; LPO, lateral preoptic area; LS, lateral septal nucleus; MeAD, medial amygdaloid nucleus, anterodorsal part; MeAV, medial amygdaloid nucleus, anteroventral part; MePD, medial amygdaloid nucleus, posterodorsal part; MePV, medial amygdaloid nucleus, posteroventral part; ml, medial lemniscus; MPN, medial preoptic nucleus; MPO, medial preoptic area; mt, mammillothalamic tract; OT, olfactory tubercle; ot, optic tract; PAG, periaqueductal gray; PH, posterior hypothalamic nucleus; Pi, piriform cortex; PLCo, posterolateral cortical amygdaloid nucleus; PMCo, posteromedial cortical amygdaloid nucleus; PMD, dorsal premammillary nucleus; PMV, ventral premammillary nucleus; PVH, paraventricular hypothalamic nucleus; PVHa, paraventricular hypothalamic nucleus, anterior part; PVP, posterior periventricular hypothalamic nucleus; PVT, paraventricular thalamic nucleus; RCH, retrochiasmatic area; Re, nucleus reuniens; SLEAm, sublenticular extended amygdala, medial part; sm, stria medullaris; ST, subthalamic nucleus; st, stria terminalis; SUM, supramammillary nucleus; VMH, ventromedial hypothalamic nucleus; VMHc, ventromedial hypothalamic nucleus, central part; VMHdm, ventromedial hypothalamic nucleus, dorsomedial part; VMHvl, ventromedial hypothalamic nucleus, ventrolateral part; VP, ventral pallidum.

infringing minimally on the medial part. Two injections were placed in the medial BST, one (case 752) in the anterior division, involving peripherally the lateral septal nucleus, and the other (case 762) in the posterior division. Three injections (cases 783, 784 and 785) were located in the medial preoptic nucleus spreading over the medial preoptic area. One injection (case 744) involved the retrochiasmatic area and, to a lesser degree, the ventral extent of the anterior hypothalamic nucleus, but it completely avoided the ventromedial hypothalamic nucleus. The two injections in the anterior hypothalamic nucleus (cases 770 and 771) involved primarily the central part. Finally, two injections were centered in the ventromedial hypothalamic nucleus, the rostroventral one (case 746) included mainly the anterior, central and ventrolateral parts and the caudodorsal one (case 747), the central and dorsomedial parts. The former injection also encroached peripherally on the retrochiasmatic area, and the latter on the dorsomedial hypothalamic nucleus.

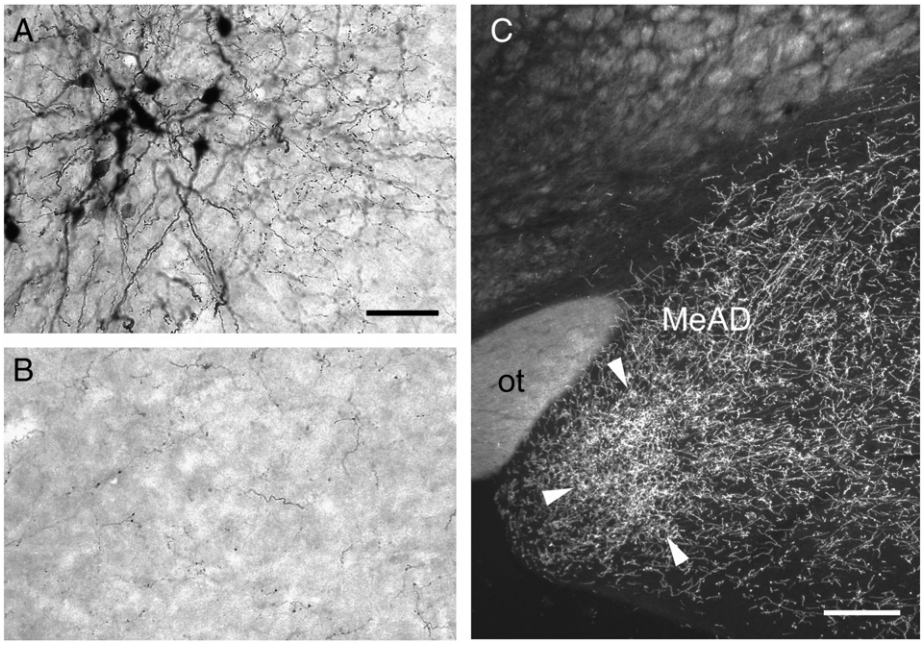

Fig. 4 – Intrinsic medial amygdaloid nucleus connections. Note the presence of a rich intraMeAV network (A) and a more modest labeling in the MePV (B) after a PHA-L injection into the MeAV (case 565), whereas a dense terminal field invests the MeAV, delimited by arrowheads, and the MeAD after a PHA-L injection into the MePV (case 765; C). Scale bar in A (applies also to B)=50 μm and in C=200 μm.

2.2.2. *Retrograde tracing observations*

In general, the control experiments fully confirmed the anterograde tracing results of the MeAV case 565. The retrograde labeling in the Me is almost exclusively ipsilateral, except after injections in the ventromedial hypothalamic nucleus where an expressive contralateral labeling is present in ventral Me parts.

A dense cluster of vividly labeled cells outlined the MeAV after injections in the lateral amygdaloid nucleus (Figs. 9A_1, 10A), posterior basomedial amygdaloid nucleus (Figs. 9A_2, 10B), amygdalostriatal transition area/lateral central nucleus (Figs. 9A_3, 10C) and ventromedial hypothalamic nucleus (Figs. 10D, 11A_4).

A moderately dense retrograde labeling was observed in the MeAV (up to 12 labeled cells per section) after injections in the retrochiasmatic area (Fig. 11A_3), anterior hypothalamic nucleus and posterior part of the medial BST (Figs. 10E, 11A_1), and a more modest one, after an injection in the anterior part of the medial BST. The substantial retrograde labeling found in the MeAV after injections in the anterior hypothalamic nucleus contrasts with PHA-L observations indicating that this nucleus contains MeAV fibers en route to more posterior targets, being itself sparingly innervated. Having in mind the possibility of an uptake of FG by fibers-of-passage (e.g., Dado et al., 1990) and of a minimal spillover of FG into adjacent parts of the ventromedial hypothalamic nucleus, one should tentatively conclude that if MeAV projections to the anterior hypothalamic nucleus do indeed exist, they are rather modest.

Very few retrogradely labeled cells (up to 3 per section) were seen in the MeAV in the three cases with injections centered the medial preoptic nucleus (Figs. 10F, 11A_2–D_2).

For comparative purpose, the retrograde labeling in the other parts of the Me will be briefly described in these FG cases (Figs. 9 and 11). In Ce/ASt case 740, a rather modest retrograde labeling was observed in the MeAD, whereas the MePV and MePD were devoid of labeling (Fig. 9A_3, B_3). In all the other FG cases, retrogradely labeled cells were distributed throughout the MeAD and MePV (Figs. 9 and 11), except for VMH cases 746 and 747, where labeled cells tended to avoid the superficial outer rim of the MePV, which reportedly expresses glutamic acid decarboxylase mRNA (Poulin et al., 2008). Retrogradely labeled MePD cells were mainly located in deeper layers and varied markedly in number in the different cases. In BSTp 762 and MPN 783 cases, a particularly heavy retrograde labeling was observed in the MePD, especially in its dorsal extent (Figs. 11C_1, D_1, C_2, D_2). In contrast, in LA 181 and BMP 737 cases, the MePD contained a much smaller number of faintly labeled cells (Figs. 9C_1, D_1, C_2, D_2).

3. Discussion

The present investigation provides the first detailed description of MeAV projections using anterograde and retrograde tract tracing techniques in the rat. The results suggest that the MeAV displays a relatively simple pattern of projections, innervating prominently a few targets it shares with the MeAD and/or the MePV, namely the ventromedial hypothalamic nucleus, especially the dorsomedial and central parts, the amygdalostriatal transition area, the lateral and posterior basomedial amygdaloid nuclei and the intraamygdaloid part of the BST. Overall, they reinforce the view that the MeAD, MeAV and MePV are interrelated and differ markedly from the MePD, as proposed by Canteras et al. (1995). Importantly, in contrast to the MeAD and MePV, the MeAV sends only

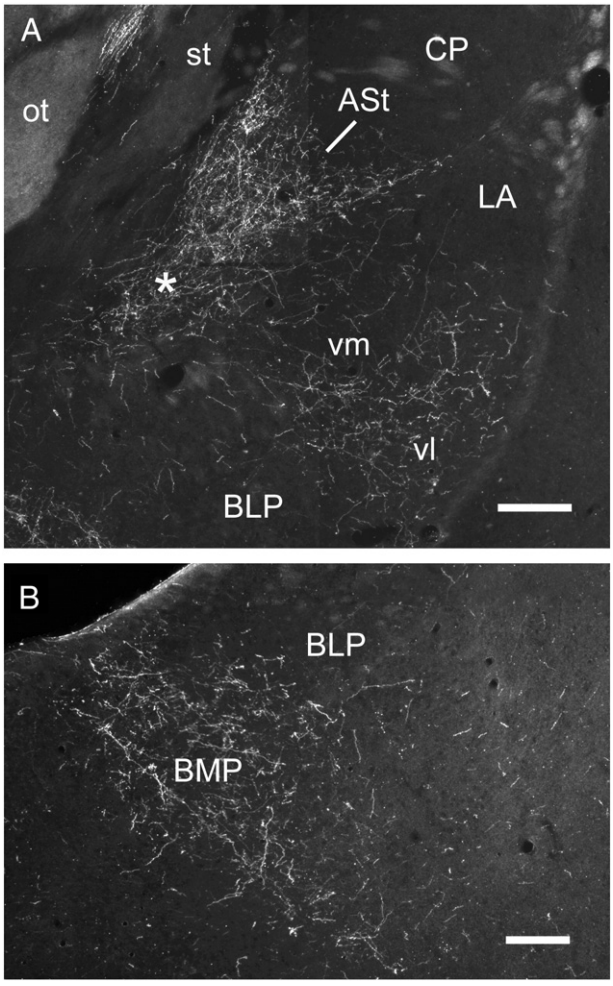

Fig. 5 – Darkfield photomicrographs of PHA-L labeling in the amygdala and amygdalostriatal transition area after an injection in the MeAV (case 565). * in A indicates the intraamygdaloid part of the bed nucleus of the stria terminalis. LAvl, lateral amygdaloid nucleus, ventrolateral part; LAvm, lateral amygdaloid nucleus, ventromedial part. For other abbreviations see Fig. 3. Scale bars=200 μm.

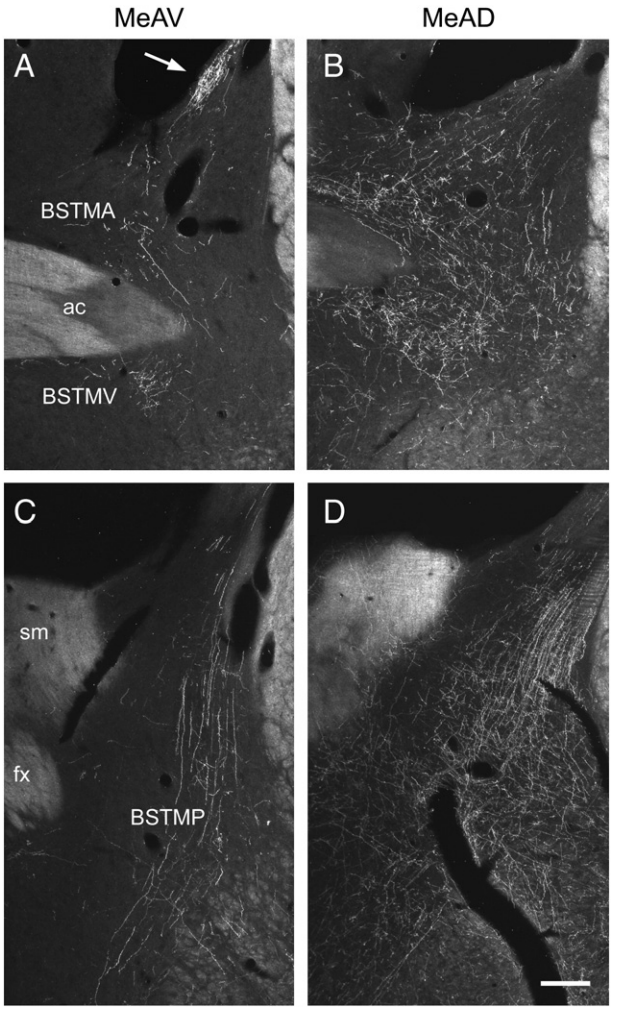

Fig. 6 – Darkfield photomicrographs of PHA-L labeling in the bed nucleus of the stria terminalis (BST) after an injection in the MeAV (case 565; A, C) and MeAD (case 517; B and D). Note that the MeAV innervates less densely the medial BST than the MeAD. In the MeAV case, labeling in the posterior division of the medial BST is located in the lateral part (C) and in the MeAD case, in the intermediate and lateral parts (D). A varicose focus apposed to the lateral ventricle, indicated by an arrow, is present only in the MeAV case (A). For abbreviations, see Fig. 3. Scale bar in D (applies all)=200 μm.

light inputs to the medial extended amygdala, main olfactory system and components of the reproductive hypothalamic network.

3.1. *Comparison with the literature*

A similar pattern of projections was observed in hamsters after Me injections restricted to the MeAD or involving the MeAD and MeAV (Coolen and Wood, 1998; Gomez and Newman, 1992) however, in rats, these injections were found to originate distinctive outputs to the ventromedial hypothalamic nucleus, ending in the shell and core (the dorsomedial and central divisions) regions, respectively (Canteras et al., 1995; present findings). The existence of a massive MeAV projection to the ventromedial hypothalamic nucleus is also supported by retrograde tracing evidence in rats (Berk and Finkelstein, 1981; present data) and mice (Choi et al., 2005). In particular, Choi et al. (2005), using exquisitely localized injections, showed in mice that MeAV neurons projecting to the ventromedial hypothalamic nucleus express the Lhx5 gene of the LIM homeodomain and target the dorsomedial rather than the ventrolateral part. Moreover, in accord with the present results, Gomez and Newman (1992) noted in a case with a PHA-L injection primarily confined to the hamster MeAV that the projections of the MeAV, although similar to, are not as extensive as those of the MeAD, particularly in view of the absence of fiber labeling in the thalamus and nucleus of the horizontal limb of the diagonal band.

The herein described MeAV projections to the posterior agranular insular, amygdalopiriform and lateral entorhinal cortices, BST, paraventricular nucleus of the hypothalamus are also supported by retrograde tracing evidence in the rat (McDonald and Jackson, 1987; Santiago and Shammah-Lagnado, 2005;

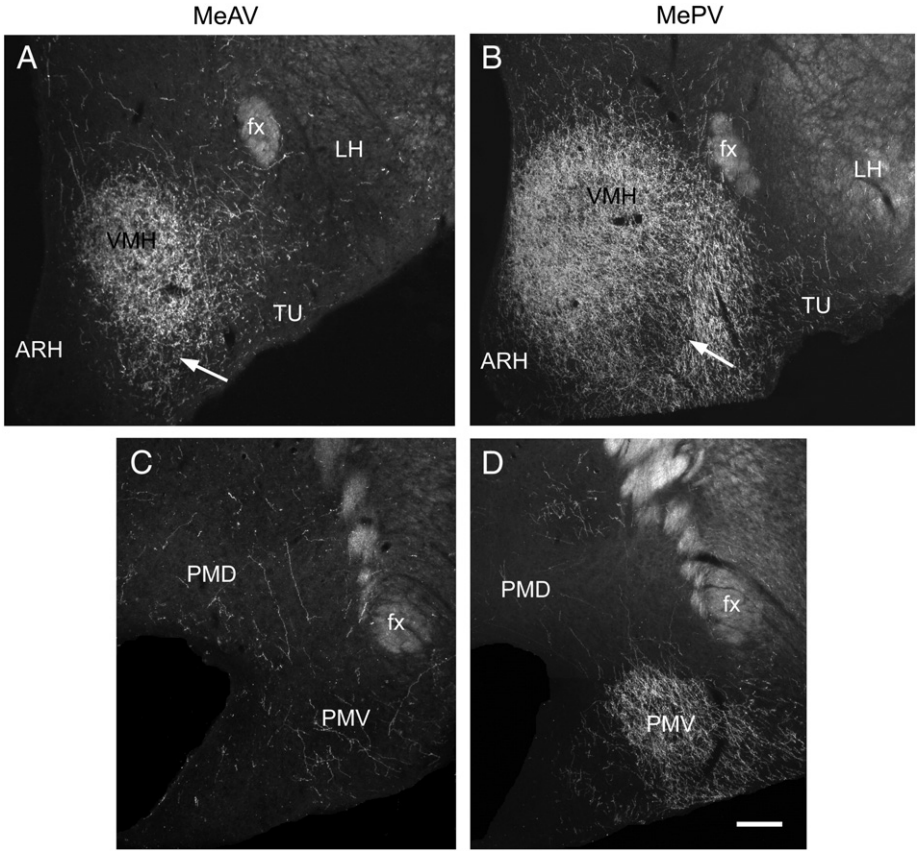

Fig. 7 – Darkfield photomicrographs of PHA-L labeling in the hypothalamus after an injection in the MeAV (case 565; A, C) and MePV (case 765; B, D). Arrows in A and B point to the ventrolateral division of the ventromedial hypothalamic nucleus. ARH, arcuate hypothalamic nucleus; Tu, tuberal hypothalamic nucleus. For other abbreviations, see Fig. 3. Scale bar in D (applies to A–D) = 200 μm.

Sawchenko and Swanson, 1983; Weller and Smith, 1982). As regards MeAV projections to the BST, it should be noted that the tiny densely varicose subventricular foci (Figs. 3A, B, 6A) do not appear to correspond in location to the ejaculation-related clusters of Fos-immunoreactive neurons documented in rodents (Coolen et al., 1996; Veening and Coolen, 1998), their functional implication being thus far unknown. Retrograde tracing observations in mice by Choi et al. (2005), in consonance with our own results, indicate that the MeAV innervates modestly the ventral premammillary nucleus and even more sparsely the medial preoptic nucleus. Having in mind that MeAV efferents also terminate rather modestly in the ventrolateral part of the ventromedial hypothalamic nucleus, and avoid almost completely the tuberal nucleus (present PHA-L observations), this scenario suggest that the MeAV exerts little if any influence on key structures of a broad hypothalamic network subserving social behaviors (Motta et al., 2009; Newman, 1999; Simerly, 2002; Swanson, 2000). Although Canteras and coworkers reliably observed retrogradely labeled cells in ventral parts of the rat Me (including the MeAV) after injections in the dorsal premammillary nucleus (Comoli et al., 2000), they argued that this labeling probably reflects a spillover of the tracer into the ventral premammillary nucleus. The present PHA-L results indicating that the MeAV provides a clear input to the dorsal premammillary nucleus are in line with anterograde tracing studies (Gomez and Newman, 1992; Luiten et al., 1985). A substantial retrograde labeling was noted in the MeAV after injections in the anterior hypothalamus (Choi et al., 2005; Price et al., 1991; our own retrograde tracing experiments), however, the present anterograde tracing observations suggest that this nucleus is essentially traversed by labeled poorly varicose passing fibers.

It should be noted that in the present study MeAV projections were examined in females, whether these projections are sexually dimorphic remain to be determined. Remarkably, in spite of the low density of receptors for gonadal hormones in the anterior Me (Simerly et al., 1990), variations in the volume of the MeAV were reported during the estrous cycle, probably related to changes in estradiol levels (Carrillo et al., 2007).

3.2. *Anatomofunctional considerations*

The possible functional significance of the MeAV is discussed based on its connectivity and on insights from studies using the expression of immediate early genes, as markers of neuronal activity (Fig. 12).

The MeAV receives robust projections from the main and accessory olfactory systems (Canteras et al., 1995; Kemppainen et al., 2002; Luskin and Price, 1983; Majak and Pitkänen, 2003;

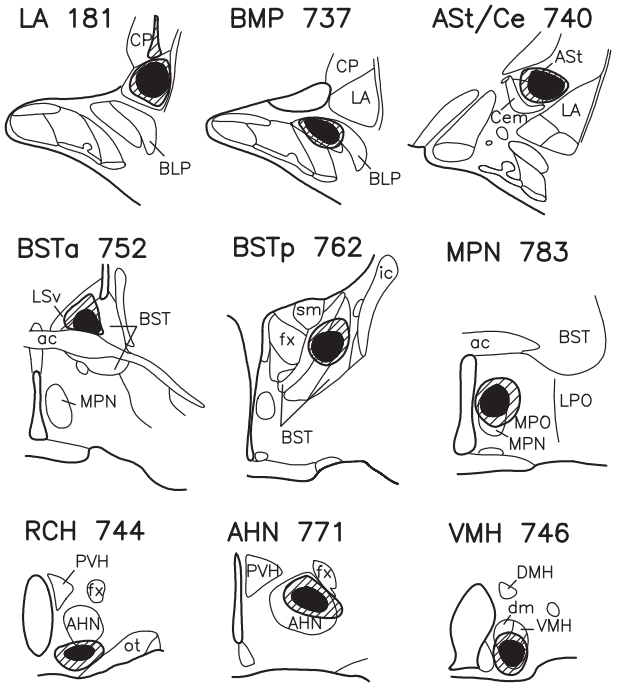

Fig. 8 – Camera lucida plots of coronal sections of representative cases indicating the core (black areas) and the surrounding halo (hatched areas) of Fluoro-Gold injections into the amygdala (LA 181, BMP 737, ASt/Ce 740), anterior and posterior divisions of the bed nucleus of the stria terminalis (BSTa 752 and BSTp 762), medial preoptic nucleus (MPN 783) and hypothalamus (RCH 744, AHN 771 and VMH 746). For abbreviations, see Fig. 3.

McDonald, 1998; Petrovich et al., 1996; Savander et al., 1996; present observations) including direct projections from the main olfactory bulb (Kang et al., 2009; Pro-Sistiaga et al., 2007; Scalia and Winans, 1975) and accessory olfactory bulb (Martinez-Marcos and Halpern, 1999; Mohedano-Moriano et al., 2007; Pro-Sistiaga et al., 2007; von Campenhausen and Mori, 2000). Axons from the accessory olfactory bulb terminate in layer I, but some also reach the deep cell layers of the MeAV, whereas in other Me parts, they are confined to layer I (Mohedano-Moriano et al., 2007; von Campenhausen and Mori, 2000). This fact suggests that direct projections from the accessory olfactory bulb to Me may exert a stronger influence on the MeAV neurons. In line with these connectional data, pharmacological stimulation of the main olfactory bulb was found to induce a robust Fos upregulation in ventral Me districts (MeAV and MePV), which was greatly reduced after the removal of the vomeronasal organ, suggesting that these Me districts are a site of convergence for the main and accessory olfactory systems (Blake and Meredith, 2010). It is interesting to note that the olfactory flow of information in the MeAV is largely unidirectional whereas the MeAD and MePV project back substantially to the main and accessory olfactory systems (Canteras et al., 1995; present observations). Another important connectional difference between the MeAV and the MeAD is that MeAV inputs originate almost exclusively from olfactory-related structures, whereas the MeAD also receives polimodal inputs from the perirhinal cortex (McDonald, 1998), ventral subiculum and lateral entorhinal cortex (Canteras and Swanson, 1992; Cullinan et al., 1993; Kishi et al., 2006; McDonald et al., 1999), lateral and posterior basomedial amygdaloid nuclei (Pitkänen, 2000) as well as inputs from the ventromedial hypothalamic and ventral

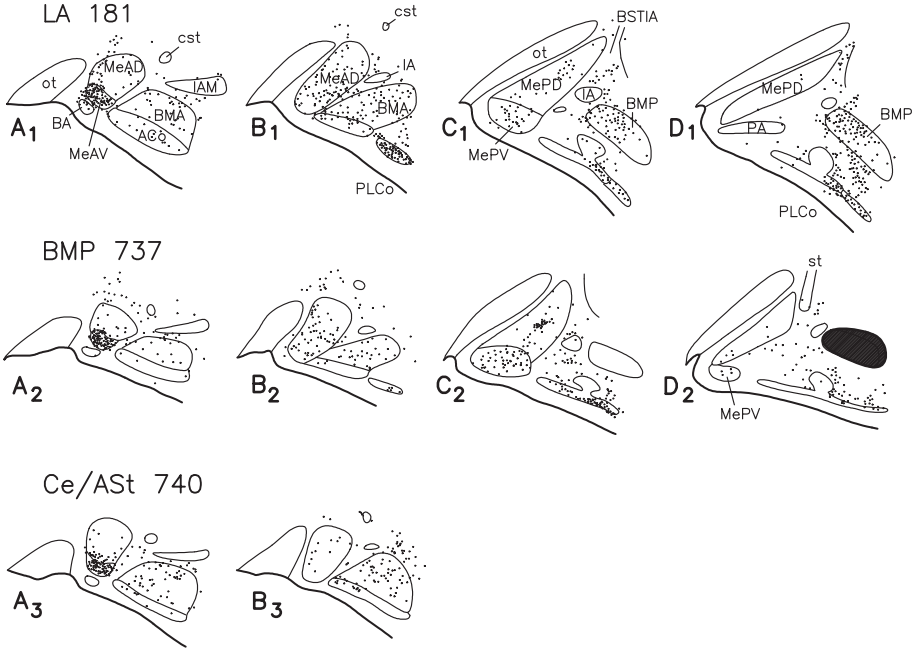

Fig. 9 – Camera lucida plots of coronal sections showing the distribution of retrogradely labeled neurons in the medial amygdaloid nucleus and adjacent districts after a FG injection into the lateral amygdaloid nucleus (LA 181), posterior basomedial amygdaloid nucleus (BMP 737) and central amygdaloid nucleus/amygdalostriatal transition area (Ce/ASt 740). The black area in D_2 indicates the FG deposit in the posterior basomedial amygdaloid nucleus. The injection sites of these cases are shown in Fig. 8. IAM, main intercalated cell mass. For other abbreviations, see Fig. 3.

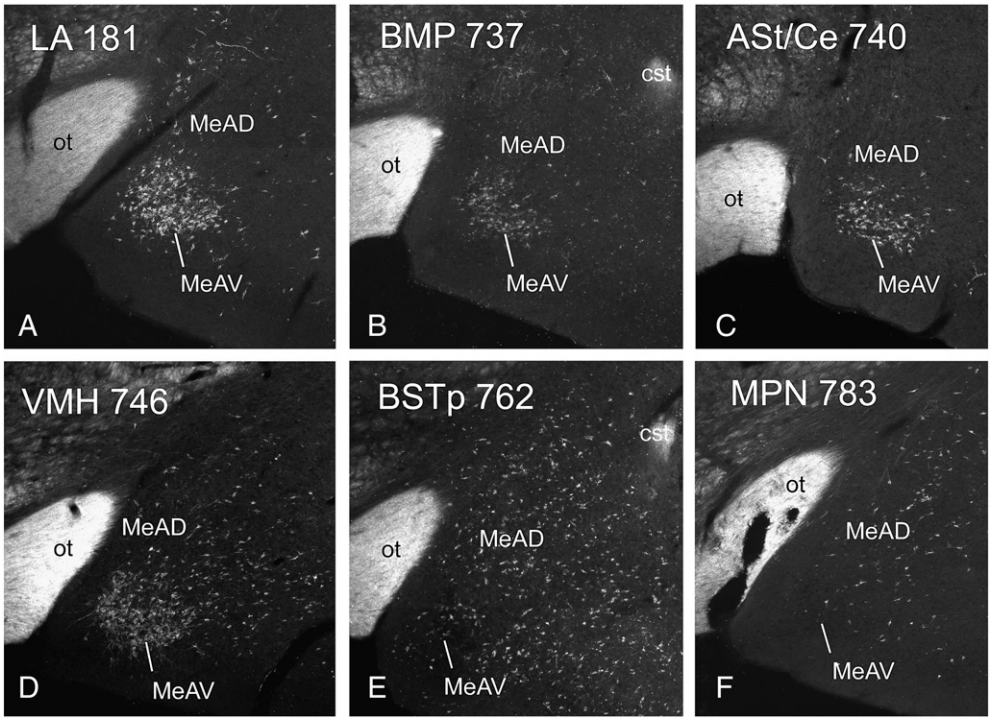

Fig. 10 – Darkfield photomicrographs showing retrogradely labeled neurons in the anterior part of the medial amygdaloid nucleus after a FG injection into the lateral amygdaloid nucleus (A), posterior basomedial amygdaloid nucleus (B), amygdalostriatal transition area/central amygdaloid nucleus (C), ventromedial hypothalamic nucleus (D), posterior division of the bed nucleus of the stria terminalis (E), and medial preoptic nucleus (F). The injection sites of these cases are shown in Fig. 8. For abbreviations, see Fig. 3. Scale bar in F (applies to A–F) = 200 μm.

premammillary nuclei, either direct or relayed by the posterior division of medial BST (Canteras et al., 1992, 1994; Dong and Swanson, 2004). It appears thus from the foregoing that the MeAV is almost exclusively influenced by chemosensory cues and acts mostly as a simple, reactive, feedforward system, lacking a recurrent hypothalamic regulation, whereas other Me parts, particularly the MeAD, are subject to a more complex modulation.

A participation of the MePV in innate anti-predator defensive responses is widely acknowledged (Canteras et al., 2001; Dielenberg et al., 2001; Motta et al., 2009). Recently, however, an increase of Fos immunolabeling was noted in other Me parts (including the MeAV) in rodents exposed to a live predator (Martinez et al., 2011) or to its odor (Samuelsen and Meredith, 2009). Importantly, connectional data reinforce a MeAV role in defensive behavior. Besides a major output to the dorsomedial part of the ventromedial hypothalamic nucleus, the MeAV also innervates the ventrolateral part of the dorsal premammillary nucleus, posterolateral part of the medial BST—also designated interfascicular nucleus of the BST (Ju and Swanson, 1989)—, MePV, ventral part of the lateral amygdaloid nucleus and posterior basomedial amygdaloid nucleus, being of note that all of these districts are components of the anti-predatory defense circuit delineated by Canteras and coworkers (Canteras et al., 2001; Martinez et al., 2011; Motta et al., 2009). It is interesting to note that the lateral nucleus and its major intraamygdaloid target, the posterior basomedial amygdaloid nucleus, are reportedly involved in emotion-related learning and memory (LeDoux et al., 1990b; Petrovich et al., 1996), and lesions of these nuclei markedly impair conditioning responses to a predator-related context (Martinez et al., 2011). Given that the MeAV and MePV originate massive projections to the dorsomedial part of the ventromedial hypothalamic nucleus, are reciprocally connected and contain a large population of glutamatergic neurons (Poulin et al., 2008), they may exert a very powerful excitatory influence on the anti-predatory defense circuit.

In addition, the present results indicate the amygdalostriatal transition area as a main output station of the MeAV. Although this transition area and the lateral amygdaloid nucleus share many input sources, they have distinct projections and are thought to be involved in different functional realms. Both of them receive auditory, visual and somatic information from posterior thalamic nuclei (Doron and LeDoux, 1999; LeDoux et al., 1990a) and from the parietal insular and temporal cortices as well as higher order polimodal information from the perirhinal cortex (McDonald, 1998). The amygdalostriatal transition area is also a major target of the lateral and posterior basomedial amygdaloid nuclei (Jolkkonen et al., 2001). Accordingly, unimodal and polimodal units responsive to auditory, visual and/or somatic stimuli have been recorded in the lateral nucleus and amygdalostriatal transition area (Uwano et al., 1995). Projections from the medial nucleus (MeAV and MeAD parts) to the lateral nucleus and amygdalostriatal transition area provide a route by which pheromonal signals from conspecifics and also potentially threatening odors of a predator (Martinez et al., 2011; Meredith and Westberry, 2004; Samuelsen and Meredith, 2009) may be conveyed to these telencephalic territories and associated with other sensory modalities. While

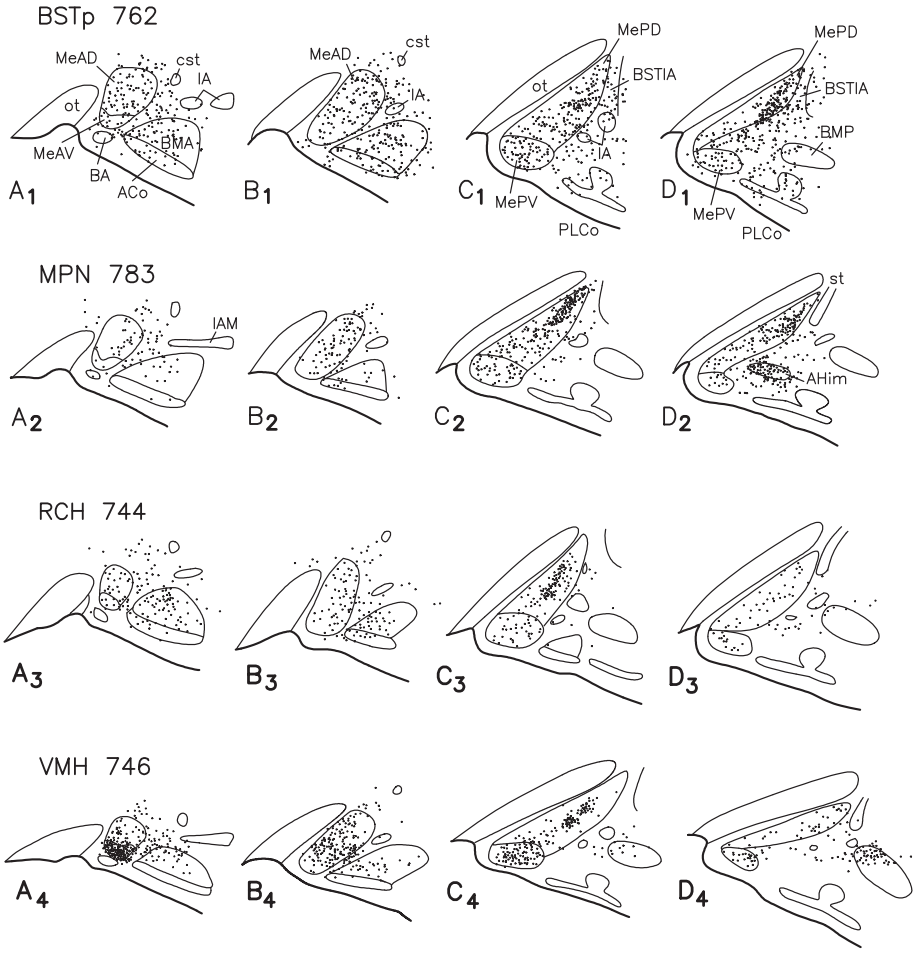

Fig. 11 – Camera lucida plots of coronal sections showing the distribution of retrogradely labeled neurons in the medial amygdaloid nucleus and adjacent districts after a FG injection into the posterior part of the bed nucleus of the stria terminalis (BSTp 762), medial preoptic nucleus (MPN 783), retrochiasmatic area (RCH 744) and ventromedial hypothalamic nucleus (VMH 746). The injection sites of these cases are shown in Fig. 8. IAM, main intercalated cell mass. For other abbreviations, see Fig. 3.

the lateral amygdaloid nucleus has extensive intraamygdaloid projections being related to emotional learning and memory (LeDoux et al., 1990b; Pitkänen, 2000), the amygdalostriatal transition area, via its projections to the caudoventral part of the globus pallidus and the substantia nigra, pars lateralis (Jolkkonen et al., 2001; LeDoux et al., 1990a; Shammah-Lagnado et al., 1996, 1999), may influence the deep layers of the superior colliculus and the external nucleus of the inferior colliculus and thereby be implicated in orienting responses to salient environmental stimuli (Doron and LeDoux,

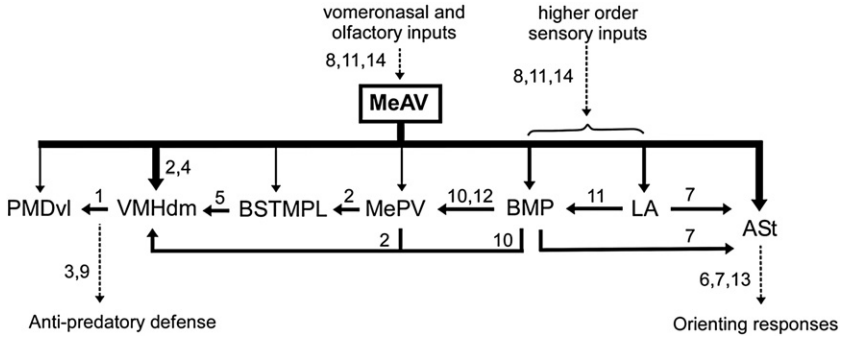

Fig. 12 – Summary of the MeAV network and its possible functional correlates. The density of each MeAV projection is roughly proportional to the thickness of the line representing it. References: 1. Canteras et al. (1994); 2. Canteras et al. (1995); 3. Canteras et al. (2001); 4. Choi et al. (2005); 5. Dong and Swanson (2004); 6. Doron and LeDoux (1999); 7. Jolkkonen et al. (2001); 8. McDonald (1998); 9. Motta et al. (2009); 10. Petrovich et al. (1996); 11. Pitkänen (2000); 12. Savander et al. (1996); 13. Shammah-Lagnado et al. (1999); 14. Swanson and Petrovich (1998). For abbreviations, see Fig. 3.

1999; Jolkkonen et al., 2001; Shammah-Lagnado et al., 1999). In line with this proposal, it has been reported that single units in the amygdalostriatal transition area, in contrast to those of the basolateral amygdaloid complex, do not display conditioned learning and other plastic responses (Toyomitsu et al., 2002; Uwano et al., 1995).

In summary, MeAV projections are a subset of those arising from the MeAD and MePV. Their major outputs to the amygdalostriatal transition area and to the dorsomedial and central parts of the ventromedial hypothalamic nucleus suggest that the MeAV may play a role in orienting responses to chemosensory cues and defensive behaviors elicited by the odor of predators.

4. Experimental procedures

Part of the material examined in this study was collected from a large library of cases used in previous investigations. The experiments were conducted on adult female Wistar albino rats weighing 170–210 g (n=40). The animals were housed in groups of four in standard polypropylene cages with food and water *ad libitum* and maintained under controlled environmental conditions (21±1 °C, 12-hour light–dark cycle with lights on at 6 am). The surgical procedures were performed under general anesthesia with a solution containing ketamine hydrochloride (Vetbrands, São Paulo, Brazil; 9 mg/100 g, i.p.) and xylazine (Vetbrands, São Paulo, Brazil; 1 mg/100 g, i.p.). Animal care and all the experimental protocols were approved by the local Animal Research Committee and are in accordance with the U.S. National Institutes of Health *Guidelines for the Care and Use of Laboratory Animals*.

4.1. *Tracer injections*

Unilateral injections of PHA-L (Vector, Burlingame, CA; 2.5% in 0.1 M sodium phosphate buffer (PB), pH 7.4) were placed stereotaxically in different parts of the Me (n=14) and of FG (Fluorochrome, Denver, CO; 2% in saline), in major targets of the Me, including the lateral amygdaloid nucleus (n=1), posterior basomedial amygdaloid nucleus (n=2), amygdalostriatal transition area (n=2), BST (n=6), medial preoptic nucleus (n=5), anterior hypothalamic nucleus (n=5) or ventromedial hypothalamic nucleus (n=5). The tracers were delivered by iontophoresis through a glass micropipette with an internal tip diameter of 10–15 μm for PHA-L and 20–25 μm for FG, by passing a positive-pulsed current, 7 s on/off intervals, set at 5 μA for 10–15 min with PHA-L, or at 1.5 μA for 5–10 min with FG. To reduce the leakage of tracer along the pipette track, the pipette was left in place for an additional 10–15 min period.

4.2. *Fixation of brains and immunohistochemistry*

After a survival of 10–14 days for PHA-L injections and 5–10 days for FG injections, the rats were deeply anesthetized and perfused transcardially by the aid of a peristaltic pump with a brief saline rinse followed by ice-cold 4% paraformaldehyde in 0.1 M PB (up to 500 ml for 30 min). Several hours later, the brains were removed from the skull, cryoprotected by overnight immersion in a 20% sucrose solution in PB at 4 °C and sectioned in the coronal plane at 40 μm into four series on a sliding microtome.

One or two series of sections were processed by immunohistochemistry by using the avidin–biotin–peroxidase (ABC) technique. The sections were incubated with a polyclonal anti-PHA-L raised in rabbit (Dako, Carpenteria, CA; diluted 1:5000 in PB containing 0.3% Triton X-100 and 10% skimmed milk) or a polyclonal anti-FG raised in rabbit (Bioscience Research Reagents, Temecula, CA; diluted 1:10,000 in PB containing 0.3% Triton X-100 and 10% skimmed milk) for 24–48 h at 4 °C. After several rinses, they were transferred to a biotinylated anti-rabbit secondary antibody raised in goat (Vector, Burlingame, CA; 1:200 dilution) for 2 h at room temperature, rinsed again and exposed to the ABC mixture (Vectastain, Elite ABC Kit, Vector Laboratories; 1:200 dilution) for 2 h at room temperature. The peroxidase reaction product was visualized by using the glucose-oxidase procedure (Itoh et al., 1979) and the metal-free 3,3′-diaminobenzidine tetrahydrochloride (DAB) as the chromogen. The sections were mounted on gelatinized slides, air-dried, and dipped in a 0.05% aqueous solution of osmium tetroxide for 20 s to enhance the visibility of the labeling, dehydrated, transferred into xylene and coverslipped with DPX. An adjacent series was stained with thionin.

4.3. *Data analysis*

The brain sections were analyzed with a microscope under brightfield and darkfield illumination. The PHA-L and FG injection sites and the distribution of anterograde labeling of representative cases were mapped by the aid of a computer drawing program (AutoCad, Release 13) combined with a microscope (Leitz, Diaplan, Leica Microsystems, Wetzlar, Germany) and camera lucida aimed at a flat-screen computer monitor. Photomicrographs were taken with a Spot 2 digital camera. The low power photomicrographs are montages of four fields captured with a ×10 objective. The digitized images were converted to gray scale and contrast and brightness adjusted by using Photoshop software (version 5.5; Adobe Systems, Mountain View, CA, USA). Unless, otherwise specified, the nomenclature and cytoarchitectonic parceling adhere to the rat brain atlas of Paxinos and Watson (2007).

Acknowledgments

We thank Dr. Martin A. Metzger and Dr. Newton S. Canteras for critical reading of a previous version of the manuscript and valuable suggestions, and Ana Maria Peraçoli Campos for expert technical assistance. We are also grateful to Dr. Newton S. Canteras for allowing us full access to his collection of cases with PHA-L injection in the medial amygdaloid nucleus. This work was supported by FAPESP grant 2008/52907-1 (to S.J.S.L) and FAPESP fellowship 2008/50445-0 (to L.S.N).

REFERENCES

Alheid, G.F., Heimer, L., 1988. New perspectives in basal forebrain organization of special relevance for neuropsychiatric disorders: the striatopallidal, amygdaloid and corticopetal components of substantia innominata. Neuroscience 27, 1–39.

Berk, M.L., Finkelstein, J.A., 1981. Afferent projections to the preoptic area and hypothalamic regions in the rat brain. Neuroscience 6, 1601–1624.

Blake, C.B., Meredith, M., 2010. Selective enhancement of main olfactory input to the medial amygdala by GnRH. Brain Res. 1317, 46–59.

Canteras, N.S., Swanson, L.W., 1992. Projections of the ventral subiculum to the amygdala, septum, and hypothalamus: a PHAL anterograde tract-tracing study in the rat. J. Comp. Neurol. 324, 180–194.

Canteras, N.S., Simerly, R.B., Swanson, L.W., 1992. Projections of the ventral premammillary nucleus. J. Comp. Neurol. 324, 195–212.

Canteras, N.S., Simerly, R.B., Swanson, L.W., 1994. Organization of projections from the ventromedial nucleus of the hypothalamus: a *Phaseolus vulgaris*-leucoagglutinin study in the rat. J. Comp. Neurol. 348, 41–79.

Canteras, N.S., Simerly, R.B., Swanson, L.W., 1995. Organization of projections from the medial nucleus of the amygdala: a PHAL study in the rat. J. Comp. Neurol. 360, 213–245.

Canteras, N.S., Ribeiro-Barbosa, E.R., Comoli, E., 2001. Tracing from the dorsal premammillary nucleus prosencephalic systems involved in the organization of innate fear responses. Neurosci. Biobehav. Rev. 25, 661–668.

Carrillo, B., Pinos, H., Guillamon, A., Panzica, G., Collado, P., 2007. Morphometrical and neurochemical changes in the anteroventral subdivision of the rat medial amygdala during estrous cycle. Brain Res. 1150, 83–93.

Choi, G.B., Dong, H.W., Murphy, A.J., Valenzuela, D.M., Yancopoulos, G.D., Swanson, L.W., Anderson, D.J., 2005. Lhx6 delineates a pathway mediating innate reproductive behaviors from the amygdala to the hypothalamus. Neuron 46, 647–660.

Comoli, E., Ribeiro-Barbosa, E.R., Canteras, N.S., 2000. Afferent connections of the dorsal premammillary nucleus. J. Comp. Neurol. 423, 83–98.

Coolen, L.M., Wood, R.I., 1998. Bidirectional connections of the medial amygdaloid nucleus in the Syrian hamster brain: simultaneous anterograde and retrograde tract tracing. J. Comp. Neurol. 399, 189–209.

Coolen, L.M., Peters, H.J.P.W., Veening, J.G., 1996. Fos immunoreactivity in the rat brain following consummatory elements of sexual behavior: a sex comparison. Brain Res. 738, 67–82.

Cullinan, W.E., Herman, J.P., Watson, S.J., 1993. Ventral subicular interaction with the hypothalamic paraventricular nucleus: evidence for a relay in the bed nucleus of the stria terminalis. J. Comp. Neurol. 332, 1–20.

Dado, R.J., Burstein, R., Cliffer, K.D., Giesler Jr., G.J., 1990. Evidence that Fluoro-Gold can be transported avidly through fibers of passage. Brain Res. 533, 329–333.

de Olmos, J.S., Heimer, L., 1999. The concepts of the ventral striatopallidal system and extended amygdala. Ann. N. Y. Acad. Sci. 877, 1–32.

de Olmos, J., Hardy, H., Heimer, L., 1978. The afferent connections of the main and the accessory olfactory bulb formations in the rat: an experimental HRP-study. J. Comp. Neurol. 181, 213–244.

Dielenberg, R.A., Hunt, G.E., McGregor, I.S., 2001. "When a rat smells a cat": the distribution of Fos immunoreactivity in rat brain following exposure to a predatory odor. Neuroscience 104, 1085–1097.

Dong, H.W., Swanson, L.W., 2004. Projections from bed nuclei of the stria terminalis, posterior division: implications for cerebral hemisphere regulation of defensive and reproductive behaviors. J. Comp. Neurol. 471, 396–433.

Doron, N.N., LeDoux, J.E., 1999. Organization of projections to the lateral amygdala from auditory and visual areas of the thalamus in the rat. J. Comp. Neurol. 412, 383–409.

Gomez, D.M., Newman, S.W., 1992. Differential projections of the anterior and posterior regions of the medial amygdaloid nucleus in the Syrian hamster. J. Comp. Neurol. 317, 195–218.

Itoh, K., Konishi, A., Nomura, S., Mizuno, N., Nakamura, Y., Sugimoto, T., 1979. Application of coupled oxidation reaction to electron microscopic demonstration of horseradish peroxidase: cobalt–glucose oxidase method. Brain Res. 175, 341–346.

Jolkkonen, E., Pikkarainen, M., Kemppainen, S., Pitkänen, A., 2001. Interconnectivity between the amygdaloid complex and the amygdalostriatal transition area: a PHA-L study in rat. J. Comp. Neurol. 431, 39–58.

Ju, G., Swanson, L.W., 1989. Studies on the cellular architecture of the bed nuclei of the stria terminalis in the rat: I. Cytoarchitecture. J. Comp. Neurol. 280, 587–602.

Kang, N., Baum, M.J., Cherry, J.A., 2009. A direct main olfactory bulb projection to the 'vomeronasal' amygdala in female mice selectively responds to volatile pheromones from males. Eur. J. Neurosci. 29, 624–634.

Kemppainen, S., Jolkkonen, E., Pitkänen, A., 2002. Projections from the posterior cortical nucleus of the amygdala to the hippocampal formation and parahippocampal region in rat. Hippocampus 12, 735–755.

Kishi, T., Tsumori, T., Yokota, S., Yasui, Y., 2006. Topographical projection from the hippocampal formation to the amygdala: a combined anterograde and retrograde tracing study in the rat. J. Comp. Neurol. 496, 349–368.

Kollack-Walker, S., Newman, S.W., 1995. Mating and agonistic behavior produce different patterns of Fos immunolabeling in the male Syrian hamster brain. Neuroscience 66, 721–736.

LeDoux, J.E., Farb, C., Ruggiero, D.A., 1990a. Topographic organization of neurons in the acoustic thalamus that project to the amygdala. J. Neurosci. 10, 1043–1054.

LeDoux, J.E., Cicchetti, P., Xagoraris, A., Romanski, L.M., 1990b. The lateral amygdaloid nucleus: sensory interface of the amygdala in fear conditioning. J. Neurosci. 10, 1062–1069.

Luiten, P.G., Koolhaas, J.M., de Boer, S., Koopmans, S.J., 1985. The cortico-medial amygdala in the central nervous system organization of agonistic behavior. Brain Res. 332, 283–297.

Luskin, M.B., Price, J.L., 1983. The topographic organization of associational fibers of the olfactory system in the rat, including centrifugal fibers to the olfactory bulb. J. Comp. Neurol. 216, 264–291.

Majak, K., Pitkänen, A., 2003. Projections from the periamygdaloid cortex to the amygdaloid complex, the hippocampal formation, and the parahippocampal region: a PHA-L study in the rat. Hippocampus 13, 922–942.

Martinez, R.C., Carvalho-Netto, E.F., Ribeiro-Barbosa, E.R., Baldo, M.V., Canteras, N.S., 2011. Amygdalar roles during exposure to a live predator and to a predator-associated context. Neuroscience 172, 314–328.

Martinez-Marcos, A., Halpern, M., 1999. Differential projections from the anterior and posterior divisions of the accessory olfactory bulb to the medial amygdala in the opossum, *Monodelphis domestica*. Eur. J. Neurosci. 11, 3789–3799.

McDonald, A.J., 1998. Cortical pathways to the mammalian amygdala. Prog. Neurobiol. 55, 257–332.

McDonald, A.J., Jackson, T.R., 1987. Amygdaloid connections with posterior insular and temporal cortical areas in the rat. J. Comp. Neurol. 262, 59–77.

McDonald, A.J., Payne, D.R., Mascagni, F., 1993. Identification of putative nitric oxide producing neurons in the rat amygdala using NADPH-diaphorase histochemistry. Neuroscience 52, 97–106.

McDonald, A.J., Shammah-Lagnado, S.J., Shi, C.J., Davis, M., 1999. Cortical afferents to the extended amygdala. Ann. N. Y. Acad. Sci. 877, 309–338.

Meredith, M., Westberry, J.M., 2004. Distinctive responses in the medial amygdala to same-species and different-species pheromones. J. Neurosci. 24, 5719–5725.

Moga, M.M., Saper, C.B., Gray, T.S., 1989. Bed nucleus of the stria terminalis: cytoarchitecture, immunohistochemistry, and

projection to the parabrachial nucleus in the rat. J. Comp. Neurol. 283, 315–332.
Mohedano-Moriano, A., Pro-Sistiaga, P., Ubeda-Banon, I., Crespo, C., Insausti, R., Martinez-Marcos, A., 2007. Segregated pathways to the vomeronasal amygdala: differential projections from the anterior and posterior divisions of the accessory olfactory bulb. Eur. J. Neurosci. 25, 2065–2080.
Motta, S.C., Goto, M., Gouveia, F.V., Baldo, M.V., Canteras, N.S., Swanson, L.W., 2009. Dissecting the brain's fear system reveals the hypothalamus is critical for responding in subordinate conspecific intruders. Proc. Natl. Acad. Sci. U.S.A. 106, 4870–4875.
Newman, S.W., 1999. The medial extended amygdala in male reproductive behavior. A node in the mammalian social behavior network. Ann. N. Y. Acad. Sci. 877, 242–257.
Paxinos, G., Watson, C., 2007. The Rat Brain in Stereotaxic Coordinates, Sixth edition. Elsevier, Amsterdam.
Petrovich, G.D., Risold, P.Y., Swanson, L.W., 1996. Organization of projections from the basomedial nucleus of the amygdala: a PHAL study in the rat. J. Comp. Neurol. 374, 387–420.
Pitkänen, A., 2000. Connectivity of the rat amygdaloid complex, In: Aggleton, J.P. (Ed.), The Amygdala, Second edition. Oxford University Press, New York, pp. 31–115.
Poulin, J.F., Castonguay-Lebel, Z., Laforest, S., Drolet, G., 2008. Enkephalin co-expression with classic neurotransmitters in the amygdaloid complex of the rat. J. Comp. Neurol. 506, 943–959.
Price, J.L., Slotnick, B.M., Revial, M.F., 1991. Olfactory projections to the hypothalamus. J. Comp. Neurol. 306, 447–461.
Pro-Sistiaga, P., Mohedano-Moriano, A., Ubeda-Banon, I., Mar Arroyo-Jimenez, M., Marcos, P., Artacho-Perula, E., Crespo, C., Insausti, R., Martinez-Marcos, A., 2007. Convergence of olfactory and vomeronasal projections in the rat basal telencephalon. J. Comp. Neurol. 504, 346–362.
Samuelsen, C.L., Meredith, M., 2009. Categorization of biologically relevant chemical signals in the medial amygdala. Brain Res. 1263, 33–42.
Santiago, A.C., Shammah-Lagnado, S.J., 2005. Afferent connections of the amygdalopiriform transition area in the rat. J. Comp. Neurol. 489, 349–371.
Savander, V., Go, C.G., LeDoux, J.E., Pitkänen, A., 1996. Intrinsic connections of the rat amygdaloid complex: projections originating in the accessory basal nucleus. J. Comp. Neurol. 374, 291–313.
Sawchenko, P.E., Swanson, L.W., 1983. The organization of forebrain afferents to the paraventricular and supraoptic nuclei of the rat. J. Comp. Neurol. 218, 121–144.
Scalia, R., Winans, S.S., 1975. The differential projections of the olfactory bulb and accessory olfactory bulb in mammals. J. Comp. Neurol. 16, 31–56.
Shammah-Lagnado, S.J., Alheid, G.F., Heimer, L., 1996. Efferent connections of the caudal part of the globus pallidus in the rat. J. Comp. Neurol. 376, 489–507.
Shammah-Lagnado, S.J., Alheid, G.F., Heimer, L., 1999. Afferent connections of the interstitial nucleus of the posterior limb of the anterior commissure and adjacent amygdalostriatal transition area in the rat. Neuroscience 94, 1097–1123.
Simerly, R.B., 2002. Wired for reproduction: organization and development of sexually dimorphic circuits in the mammalian forebrain. Annu. Rev. Neurosci. 25, 507–536.
Simerly, R.B., Chang, C., Muramatsu, M., Swanson, L.W., 1990. Distribution of androgen and estrogen receptor mRNA-containing cells in the rat brain: an in situ hybridization study. J. Comp. Neurol. 294, 76–95.
Swanson, L.W., 2000. Cerebral hemisphere regulation of motivated behavior. Brain Res. 886, 113–164.
Swanson, L.W., Petrovich, G.D., 1998. What is the amygdala? Trends Neurosci. 21, 323–331.
Toyomitsu, Y., Nishijo, H., Uwano, T., Kuratsu, J., Ono, T., 2002. Neuronal responses of the rat amygdala during extinction and reassociation learning in elementary and configural associative tasks. Eur. J. Neurosci. 15, 753–768.
Uwano, T., Nishijo, H., Ono, T., Tamura, R., 1995. Neuronal responsiveness to various sensory stimuli, and associative learning in the rat amygdala. Neuroscience 68, 339–361.
Veening, J.G., Coolen, L.M., 1998. Neural activation following sexual behavior in the male and female rat brain. Behav. Brain Res. 92, 181–193.
von Campenhausen, H., Mori, K., 2000. Convergence of segregated pheromonal pathways from the accessory olfactory bulb to the cortex in the mouse. Eur. J. Neurosci. 12, 33–46.
Weller, K.L., Smith, D.A., 1982. Afferent connections to the bed nucleus of the stria terminalis. Brain Res. 232, 255–270.